

# On the effect of tidal flats on the hydrodynamics of the Tagus estuary

André B. FORTUNATO <sup>a</sup>, Anabela OLIVEIRA <sup>a</sup>, António M. BAPTISTA <sup>b</sup>

<sup>a</sup> Laboratório Nacional de Engenharia Civil, Departamento de Hidráulica, Núcleo de Estuários, Av. do Brasil 101, 1799 Lisboa Codex, Portugal

<sup>b</sup> Oregon Graduate Institute of Science & Technology, Center for Coastal and Land-Margin Research, P.O. Box 91000 Portland, OR 97291-1000, USA

(Received 20 May 1997, revised 6 October 1997, accepted 5 December 1997)

**Abstract** – The effects of tidal flats on the hydrodynamics of the Tagus estuary are analysed using an accurate high-resolution shallow water model, supported by field data. Tidal flats act mainly as energy filters, rather than sinks, transferring energy from astronomic to non-linear frequencies. They also play a major role in determining the strong resonance mode that amplifies semi-diurnal constituents. We show that the upper estuary, with extensive tidal flats, has an increasing accretion rate. This “filling-up” results from a positive feedback between sediment deposition and the hydrodynamics: accretion in the upper estuary lengthens the duration of ebbs, decreasing sediment flushing and further increasing accretion. © Elsevier, Paris / Ifremer / Cnrs / Ird

**tidal flats / tidal propagation / numerical model / Tagus estuary**

**Résumé** – Sur l'effet des estrans sur l'hydrodynamique de l'estuaire du Tage. Les effets des estrans sur l'hydrodynamique de l'estuaire du Tage sont analysés à travers un modèle d'écoulement de haute résolution, et des données de terrain. Les estrans fonctionnent surtout comme des filtres d'énergie, et non pas comme des dissipateurs, transférant l'énergie des fréquences astronomiques à des fréquences non-linéaires. Les estrans ont aussi un rôle très important dans la détermination du mode de résonance qui amplifie les constituantes semi-diurnes. Nous montrons que la partie supérieure de l'estuaire, dominée par des estrans, a un taux de sédimentation croissant. Ceci est dû à une rétro-action positive entre le dépôt de sédiments et l'hydrodynamique : le dépôt dans la partie supérieure de l'estuaire augmente la durée des reflux de marée, réduisant le transport de sédiments vers l'extérieur, et contribuant ainsi à leur accumulation dans l'estuaire. © Elsevier, Paris / Ifremer / Cnrs / Ird

**estran / propagation de marée / modèle numérique / estuaire du Tage**

## 1. INTRODUCTION

Tidal flats are an important feature of many estuaries: from a physical perspective, they slow down tidal propagation and promote mixing by tidal trapping; from an ecological perspective, they contribute significantly to primary production, and are often breeding grounds for many species. The effects of tidal flats on hydrodynamics can have repercussions on the ecosystem. For instance, enhanced mixing reduces stratification, which in turn increases the oxygen concentration near the bottom,

affecting the biological cycles. The evolution of tidal flats due to sediment deposition, land reclamation or sea level rise can therefore influence the estuary as a whole.

In this context, the Tagus estuary constitutes an interesting case study because 40 % of its area dries out at low tide, and sediment deposition is gradually changing the tidal flats [1]. Our objective is to understand the role and effect of tidal flats in and on the hydrodynamics of the Tagus estuary. Since the direct application of simplified analyses is prevented by the complex geometry of the

estuary [7], we developed an accurate numerical model to pursue our investigation.

This paper is organized as follows. In Section 2, we analyse the historical data related to the hydrodynamics of the Tagus estuary. The data are used both to set up the numerical model and to evaluate changes in the hydrodynamics over a 15-year period. Section 3 presents the development and validation of a high-resolution tidal model for the Tagus estuary. In Section 4, the model is used to investigate the effect of the tidal flats on the hydrodynamics. Section 5 summarizes the major conclusions.

2. DATA

2.1. Data Processing and Critical Assessment

The most comprehensive bathymetric survey of the estuary dates from 1964–1967, and includes information from the coastal area to Muge (about 80 km upstream). Recent updates to this database are indicated in *figure 1*. Near the mouth, some morphological changes are occurring: the Bico do Pato shoal is moving southeast and the Bugio Bank is eroding and extending northward [13]. In the upper estuary, bathymetric comparisons indicate sig-

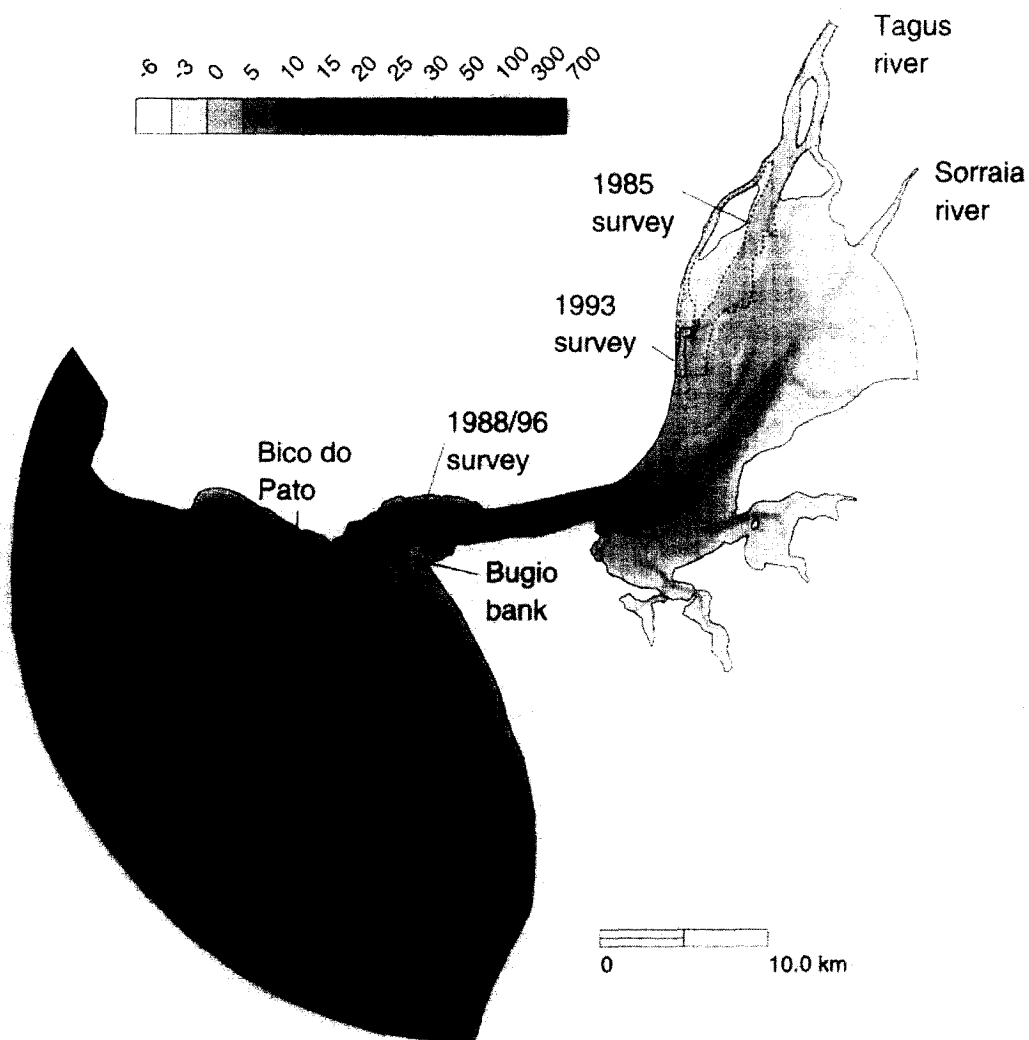


**Figure 1.** Bathymetry of the Tagus estuary, relative to the chart datum. The upper estuary is characterized by extensive tidal flats, small islands and a web of narrow channels. The lower estuary consists of a deep channel, about 12 km long and 2 km wide, that opens into a large bay. This channel is prolonged inside the bay by a canyon about 15–20 m deep delimited by two sand banks.

nificant deposition in the tidal flats [1, 6], and dredging of navigation channels is common. Our data there are thus potentially obsolete. A bathymetric database was built starting with the 1964–1967 information, using more recent surveys for updates where possible.

Extensive tidal data are available throughout the estuary. One-year-long time series of tidal elevations were measured in 1972 at fourteen stations (*figure 2*). For three stations (V.F. Xira, Lisboa and Cascais), continuous time series of tidal elevations are also available for periods of several years. Yearly time series were harmonically analysed for 53 constituents at all stations (*table 1*). Tidal data appear self-consistent for all stations except Alfeite (where, for example, the  $M_2$  phase is larger than at Seixal - *table 1*). Our numerical simulations will be performed for 1972, given the amount of data available for that year. Velocity time series, measured between 15 October and 15 November 1987 at a single point in the vertical, are available at eight stations near the mouth of the estuary (*figure 2*). These time series were harmonically analysed along the principal axes using the eleven constituents used in the model. L2-norms between raw and reconstructed time series vary between 7 and 18  $\text{cm s}^{-1}$  for

each horizontal velocity component, with an average error of 10  $\text{cm s}^{-1}$ . The data at C02 and C08 were considered unreliable and were discarded. At C02, located in the channel, the angle between velocities and the channel axis is 13 degrees. We attribute this discrepancy to the presence of a bridge pier which has a localized effect on the currents. At C08, the data is extremely noisy, leading to an L2-norm between raw and reconstructed time series of 18  $\text{cm s}^{-1}$ .

The Tagus river flow constitutes the main source of fresh-water into the estuary. Average annual flows are of the order of 400  $\text{m}^3 \text{s}^{-1}$ , while monthly averaged values vary between 40 and 4000  $\text{m}^3 \text{s}^{-1}$  [2]. Other freshwater inputs to the estuary are small and will be neglected in this study. The average annual flow in the Sorraia and the Trancão [15] amounts to about 35 and 2.5  $\text{m}^3 \text{s}^{-1}$ , respectively.

## 2.2. Data Analysis

Tides in the Tagus estuary are mainly semi-diurnal, with tidal ranges varying from 0.75 m in neap tides in Cascais to 4.3 m in spring tides in the upper estuary. The tidal

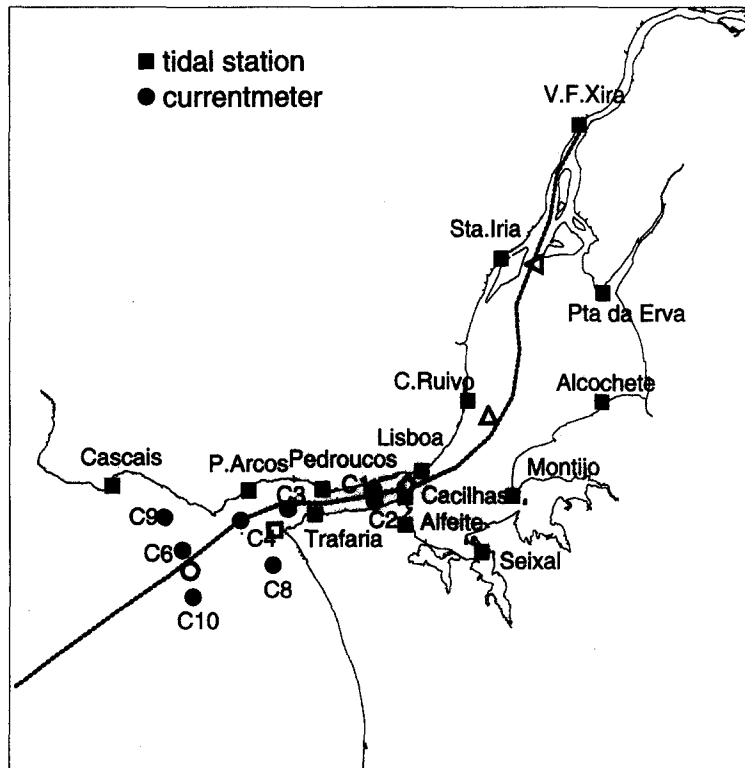


**Figure 2.** Tagus estuary: tidal and current-meter stations. The open symbols are used in *figure 8*, and the dotted line in *figure 9*.

**Table I.** Elevation amplitudes (m) and phases (rd) for the 14 tidal stations, for the constituents used in the numerical model.

Station	Constituent										
	Z <sub>0</sub>	Ms <sub>1</sub>	O <sub>1</sub>	K <sub>1</sub>	N <sub>2</sub>	M <sub>2</sub>	S <sub>2</sub>	M <sub>4</sub>	MS <sub>4</sub>	M <sub>6</sub>	2MS <sub>6</sub>
Cascais	2.154 (-)	0.008 (3.93)	0.062 (5.80)	0.072 (0.96)	0.218 (2.41)	0.954 (1.50)	0.331 (2.13)	0.012 (3.80)	0.009 (5.65)	0.002 (3.44)	0.000 (-)
P. Arcos	2.206 (-)	0.020 (2.90)	0.068 (5.99)	0.071 (0.95)	0.218 (2.60)	0.998 (1.61)	0.353 (2.51)	0.022 (5.14)	0.017 (6.01)	0.006 (4.84)	0.007 (5.55)
Trafaria	2.229 (-)	0.014 (0.41)	0.068 (6.01)	0.069 (6.01)	0.221 (2.70)	1.038 (1.67)	0.365 (2.31)	0.038 (5.16)	0.024 (6.27)	0.007 (5.61)	0.008 (6.14)
Pedrouços	2.189 (-)	0.014 (2.99)	0.069 (5.99)	0.072 (0.94)	0.215 (2.61)	1.061 (1.62)	0.371 (2.29)	0.047 (4.99)	0.031 (5.85)	0.008 (5.39)	0.010 (6.17)
Cacilhas	2.161 (-)	0.013 (3.34)	0.072 (6.03)	0.072 (0.99)	0.241 (2.69)	1.128 (1.68)	0.399 (2.35)	0.067 (4.87)	0.039 (5.75)	0.011 (5.40)	0.012 (6.18)
Lisboa	2.240 (-)	0.012 (3.07)	0.069 (6.02)	0.071 (1.00)	0.240 (2.70)	1.138 (1.69)	0.407 (2.36)	0.079 (4.93)	0.048 (5.75)	0.011 (5.73)	0.012 (0.18)
Alfeite	2.307 (-)	0.058 (0.74)	0.066 (6.25)	0.070 (1.17)	0.254 (2.93)	1.244 (1.90)	0.430 (2.63)	0.079 (5.52)	0.037 (0.51)	0.029 (5.73)	0.033 (0.23)
Seixal	2.226 (-)	0.015 (1.07)	0.070 (6.05)	0.071 (1.03)	0.242 (2.74)	1.141 (1.74)	0.408 (2.40)	0.084 (5.02)	0.045 (6.02)	0.011 (4.93)	0.013 (5.64)
Montijo	2.265 (-)	0.028 (1.02)	0.070 (6.01)	0.074 (1.03)	0.252 (2.73)	1.183 (1.72)	0.423 (2.40)	0.086 (5.08)	0.047 (6.08)	0.011 (4.71)	0.011 (5.48)
C. Ruivo	2.276 (-)	0.020 (1.20)	0.071 (6.01)	0.072 (1.04)	0.250 (2.74)	1.207 (1.74)	0.430 (2.41)	0.095 (5.12)	0.054 (6.11)	0.013 (5.17)	0.014 (5.88)
Alcochete	2.243 (-)	0.035 (0.91)	0.072 (6.06)	0.073 (1.09)	0.251 (2.87)	1.248 (1.82)	0.436 (2.53)	0.066 (5.52)	0.035 (0.58)	0.041 (4.95)	0.041 (5.70)
Sta. Iria	2.315 (-)	0.060 (0.69)	0.066 (6.26)	0.078 (1.10)	0.254 (2.93)	1.245 (1.90)	0.439 (2.65)	0.079 (5.52)	0.037 (0.51)	0.029 (5.73)	0.033 (0.05)
P. Erva	2.233 (-)	0.057 (0.89)	0.072 (6.12)	0.074 (1.15)	0.263 (2.93)	1.278 (1.88)	0.447 (2.60)	0.086 (5.57)	0.043 (0.52)	0.031 (5.57)	0.033 (0.05)
V.F. Xira	2.469 (-)	0.116 (0.88)	0.070 (0.02)	0.070 (1.36)	0.227 (3.27)	1.177 (2.17)	0.371 (2.97)	0.037 (4.02)	0.033 (3.99)	0.036 (0.65)	0.035 (1.43)

form number (ratio between amplitudes of the two main diurnal and the two main semi-diurnal constituents) varies between 0.08 and 0.10.  $M_2$  is the dominant tidal constituent, with amplitudes of the order of 1 m (table I). For semi-diurnal constituents, the phase difference between the outermost (Cascais) and the innermost (V.F. Xira) stations is about 1 h 20 min.

Amplitudes and phases of representative constituents provide a general picture of the tidal propagation inside the estuary (figure 3). The amplitudes of astronomic constituents grow rapidly in the channel and more steadily in the upper estuary, up to St. Iria, and then decrease up to V.F. Xira. This trend is especially pronounced for semi-diurnal constituents, which suggests the presence of a resonance mode with a period close to twelve hours. Shallow-water constituents are negligible in the coastal region but increase rapidly inside the estuary. Fourth-diurnal amplitudes increase strongly up to Lisbon, and then decrease in the upper estuary. The growth of  $M_4$  in the channel indi-

cates the importance of advective accelerations in this area. The importance of friction in the upper estuary is confirmed by the growth of six-diurnal constituents in that area.

Stratification conditions vary strongly with river flow and tidal conditions. The estuary is well mixed for spring tides and low river flows [12] and partially stratified for average conditions [3, 17]. Salinity differences from bottom to surface between 10 and 20 ppt were measured after a flood at several stations [12], indicating that the estuary can be strongly stratified under extreme conditions.

Since our data were collected over two decades, the changes in the estuary over that period should be assessed. The yearly evolution of the  $M_2$  at three locations reveals a clear trend at V.F. Xira: phases increase and amplitudes decline with time, unlike at the two other stations (figure 4). This result is consistent with the depo-

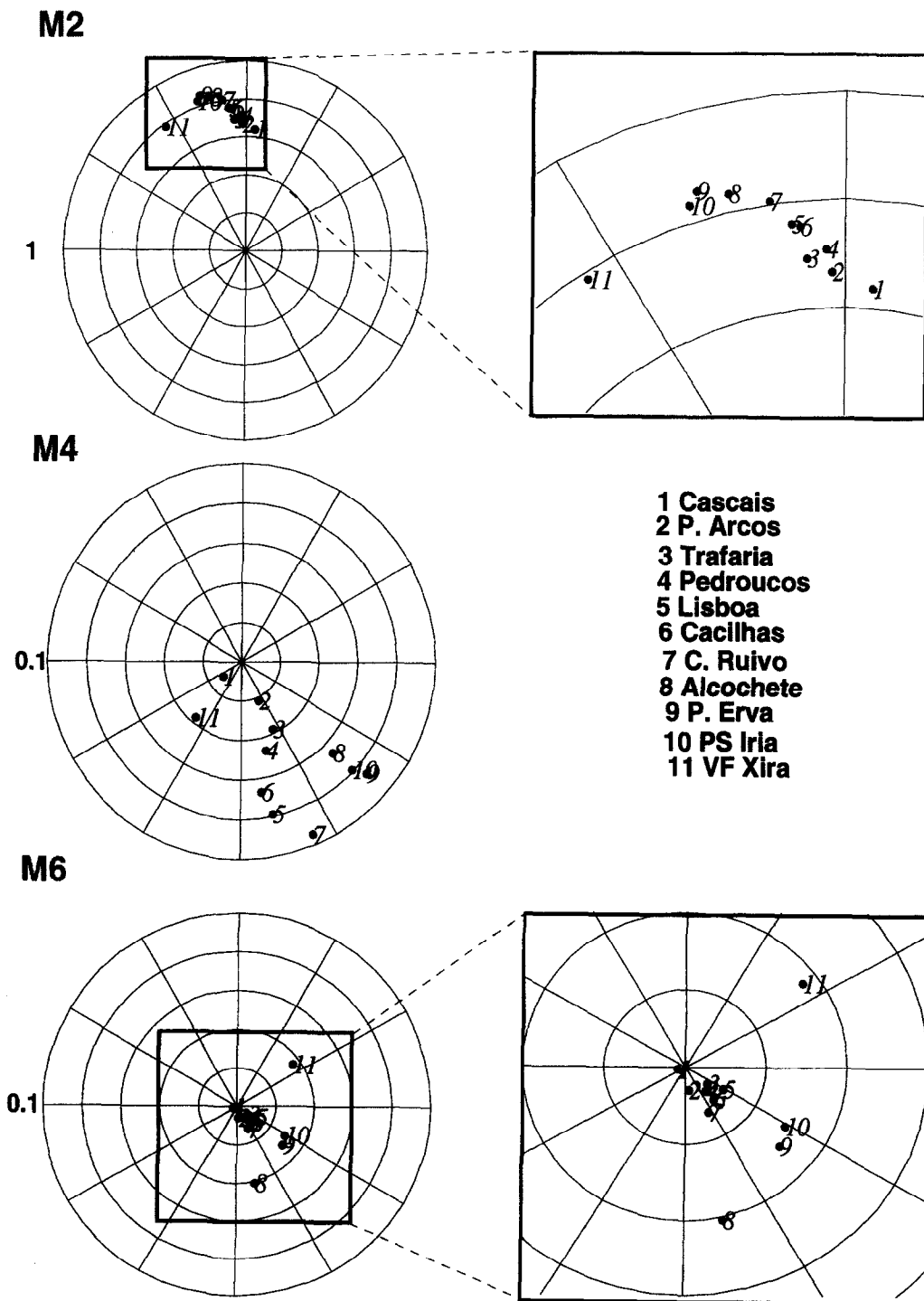


**Figure 3.** Polar representation of amplitudes and phases for  $M_2$ ,  $M_4$  and  $M_6$ ; the distance from the centre to each point represents the amplitude; the angle, measured counter-clockwise from the X-axis, represents the phase.

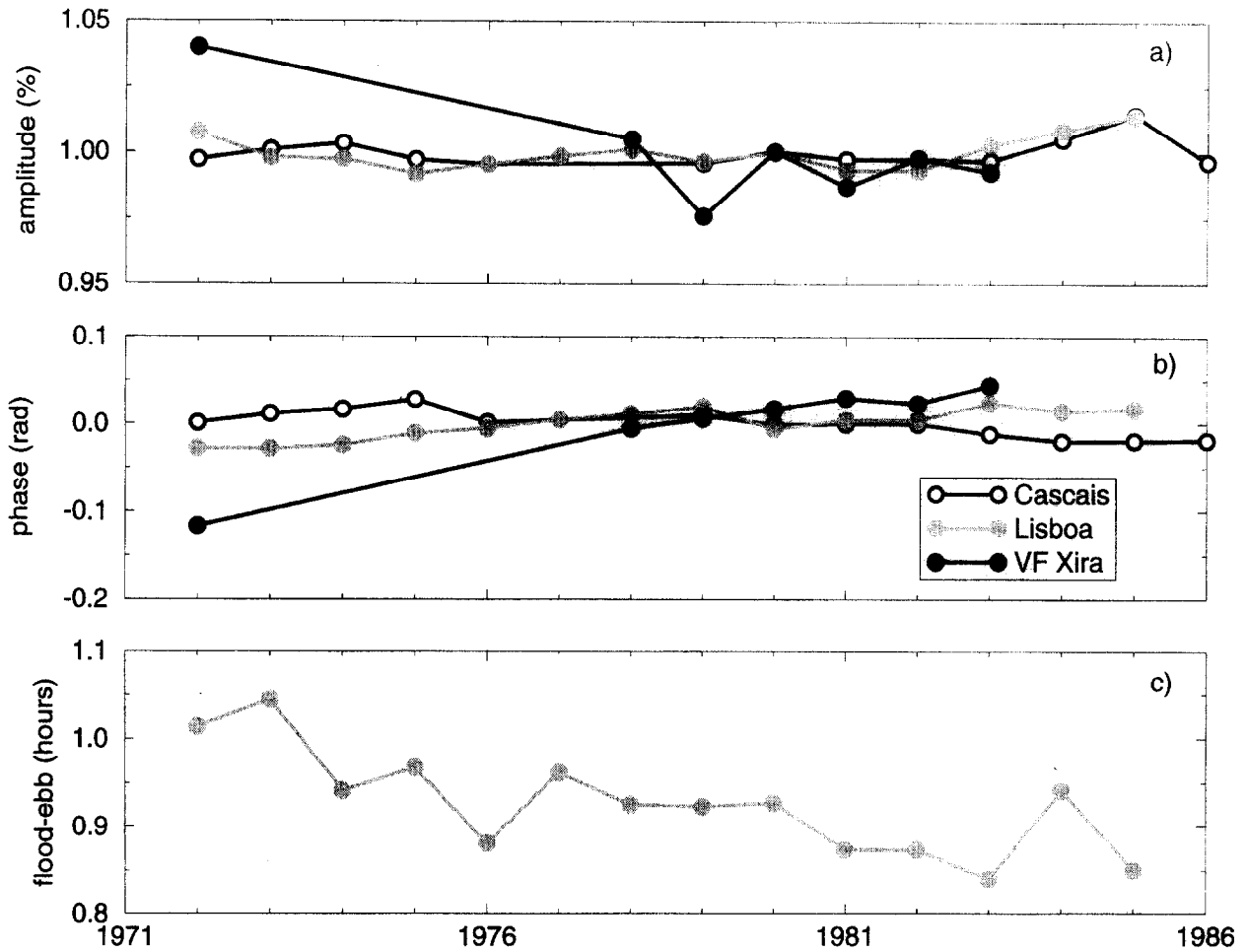


Figure 4. Yearly evolution of tides. a)  $M_2$  amplitudes; b)  $M_2$  phases; c) difference between average flood and ebb durations.

sition occurring in the upper estuary. *Figure 4* also shows that floods are typically an hour longer than ebbs [14]. This behaviour leads to stronger velocities during ebbs, and thus to a net export of sediments [7]. However, the difference in duration is decreasing by about  $40 \text{ s y}^{-1}$ , suggesting a reduction of the sediment flux into the shelf. This reduction could be partially responsible for both the erosion at the mouth of the estuary, and the accretion in the upper estuary.

### 3. MODEL APPLICATION AND ASSESSMENT

Numerical modelling of tides in the Tagus estuary involves four major difficulties: (1) the accurate represen-

tation of some narrow channels and boundaries requires horizontal resolutions of the order of tens of metres, which may lead to unacceptable computational costs; (2) advective accelerations are very important at the mouth of the estuary, potentially leading to artificial oscillations in the numerical model; (3) tidal flats must be represented because they affect tidal propagation and transport; and, (4) density gradients can affect residual currents under large river flows [17], thus a three-dimensional baroclinic model may be required for a correct representation of the hydrodynamics under extreme conditions. The shallow-water model used herein, ADCIRC [10, 11], efficiently addresses the first three difficulties: the use of finite elements allows for the correct representation of narrow channels and complex boundaries at acceptable computa-

tional costs; the generalized wave continuity equation formulation propagates and dissipates spurious modes while being extremely accurate for long physical waves; and recent versions of the model allow for wetting and drying of the nodes during the tidal cycle. The model application presented herein improves our previous work [5] by drastically increasing the horizontal resolution, and by explicitly representing the wetting and drying of tidal flats. The water column is assumed to be well-mixed, since we concentrate on average river flow conditions, thus baroclinic effects are neglected.

The grid extends from V.F. Xira to about 20 km seaward of the mouth, away from the influence of the tidal jet coming from the estuary (*figure 5*). Grid spacing, between 15 and 1500 m, decreases with the complexity of the flow (e.g. near the mouth), and the geometry (near narrow channels and complex boundaries). Boundary conditions were imposed with elevation data from V.F. Xira and Cascais, for the river and ocean boundaries, respectively. Imposing river flow, rather than elevations, at the upstream boundary would require extending the domain by about 30 km, to the limit of tidal propagation.

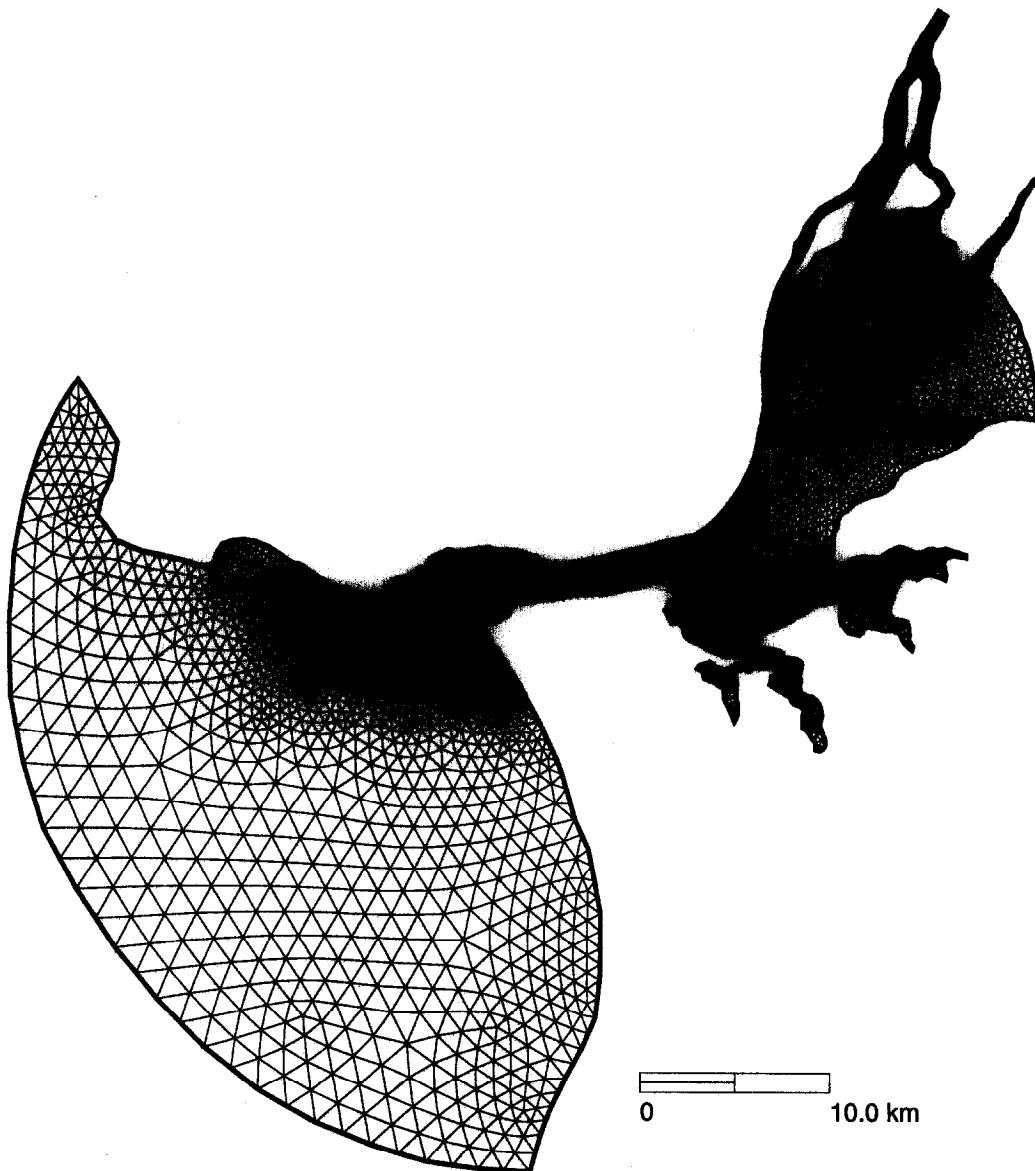


**Figure 5.** Grid for the Tagus estuary, with 31 000 elements and 16 000 nodes.

This extension was not made due to the lack of reliable bathymetric data upstream of V.F. Xira. The major 11 tidal constituents (*table 1*) were imposed, except at the ocean boundary where non-linear tidal constituents were neglected. Also, the harmonic analysis of 1972 data at Cascais leads to an amplitude of the  $S_2$  about 5 % smaller than in other years [16]. The amplitude of the  $S_2$  at the ocean boundary was therefore increased to account for an apparent data error.

The model was not calibrated for the friction coefficient. Previous calibrations of different tidal models in this system consistently led to optimal friction coefficients that were unrealistically low, and, as shown below, the same would happen in the present application. Either stratification or channel deepening could reduce frictional effects in the upper estuary and explain this phenomenon. The second explanation is consistent with the decline in amplitude of the  $M_2$  over the years in V.F. Xira (*figure 4*), since the tidal data is from 1972, and the bathymetry used at the riverine end of the estuary is from 1985. The friction coefficient was therefore specified as in previous simulations of the same system, i.e. small but within realistic values. A Manning-type formulation was used in shallow waters, with a Manning coefficient of  $0.02 \text{ m}^{1/3} \text{ s}^{-1}$ .

Runs were performed for 20 days, and results were harmonically analysed at every grid point for the final 16 days. Harmonically synthesized data and model results were used to compute elevation and velocity root-mean-square errors as:

$$RMS_e = \sqrt{\frac{1}{nt} \sum_{i=1}^{nt} (\eta_i - \tilde{\eta}_i)^2} \quad (1)$$

and,

$$RMS_v = \sqrt{\frac{1}{nt} \sum_{i=1}^{nt} \left\{ (u_i - \tilde{u}_i)^2 + (v_i - \tilde{v}_i)^2 \right\}} \quad (2)$$

where  $\eta$  is the elevation,  $u$  and  $v$  are the depth-averaged velocities, the tilde represents numerical results,  $nt = 17520$  is the number of time steps, and the time step was taken as 30 min.

Both elevations and velocities are well represented (*figure 6*): the average errors are 9 cm ( $RMS_e$ ) and  $19 \text{ cm s}^{-1}$  ( $RMS_v$ ), which represent significant reductions relative to Fortunato et al. [5].  $M_2$  tidal ellipses confirm the model accuracy (*figure 7*). As an additional verification, the river flow through the upper boundary was computed

using the model results, by harmonically analysing the normal flux. The value obtained,  $547 \text{ m}^3 \text{ s}^{-1}$  is close to the average river flow of the Tagus in 1972 ( $515 \text{ m}^3 \text{ s}^{-1}$ ). Semi-diurnal constituents are generally under-predicted, whereas sixth-diurnal constituents are over-predicted. This contrast shows that decreasing the friction coefficient would reduce the errors. This hypothesis is confirmed by the general under-prediction of  $Z_0$ : the energy loss in the shallow upper estuary rapidly reduces the mean sea level in the estuary. However, as pointed out above, reducing the friction coefficient would be an attempt to compensate for the inconsistency between the tidal and bathymetric data, and would lead to unrealistic values.

## 4. HYDRODYNAMICS

### 4.1. Tidal Propagation

The spatial distribution of individual frequencies suggests that resonance may be important in this estuary because semi-diurnal constituents in the upper estuary grow more than diurnal constituents (*table 1*). To study this hypothesis, a simplified analysis was set up by closing the domain upstream and doing several runs forced with single tidal constituents, with periods varying from 3 h to 19 h and amplitudes of one metre. A one-dimensional diagram of amplitudes along the estuary shows that there is a strong resonance mode for a period of about eight hours (*figure 8*). Resonance effects clearly explain the increased growth of the semi-diurnal constituents (about 30 %) relative to the diurnal frequencies (about 8 %).

To assess the effect of tidal flats on tidal propagation, the simulation described in the previous section (run A) was compared with a simulation without tidal flats (run B). Tidal flats were removed by eliminating all nodes with depths over 0.5 m above the chart datum. Boundary conditions were the same for both runs, making the comparison of the results near the upstream boundary meaningless. However, the effect of the upstream boundary condition is expected to decrease rapidly into the estuary, since only a small fraction of the tidal energy propagates into the riverine part of the estuary (see below). Furthermore, imposing the same boundary conditions in both runs reduces the differences between them, making our analysis conservative. Results are compared by examining the amplitudes and phases of representative constituents along a line (*figure 9*).



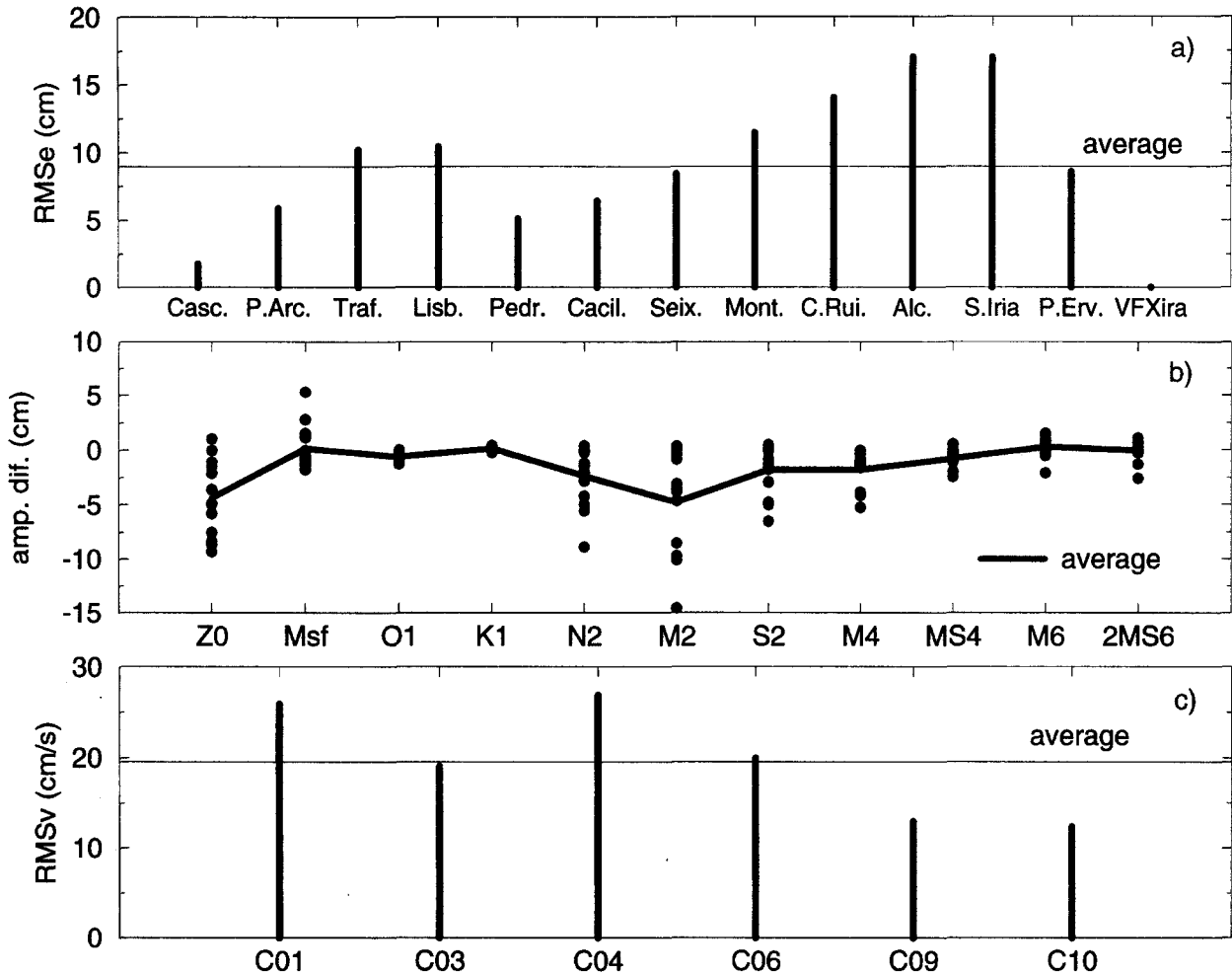


Figure 6. Model validation. a) Elevation root-mean-square errors. b) Amplitude errors. c) Velocity root-mean-square errors.

Shallow-water constituents are drastically reduced by the removal of tidal flats. This reduction has two causes. First, velocities decrease in the lower estuary due to the reduction of the volume of the estuary. The generation of even harmonics by advective accelerations, and odd harmonics by friction is therefore reduced. Secondly, the generation of even harmonics by finite amplitude and odd harmonics by friction is eliminated over the tidal flats. The comparison between the one-dimensional diagrams for  $M_4$  and  $M_6$  suggests that the velocity reduction affects mostly the even harmonics, which are primarily generated in the lower estuary, while the generation of odd harmonics is affected by both processes.

The effect of the removal of tidal flats on the astronomic constituents is due to the combination of two phenomena. On the one hand, the growth of non-linear constituents

occurs at the expense of the astronomic constituents. Removing the tidal flats reduces this generation, thereby increasing the growth of astronomic constituents. On the other hand, tidal flats affect the resonance mode of the estuary, thus affecting all constituents. The removal of tidal flats increases the average depth of the estuary, thus increasing the celerity of the waves. This increase reduces the period of the resonance mode, and reduces the amplification of tidal waves. Since the resonance period is less than twelve hours, the reduction of wave amplification will be stronger for semi-diurnal than for diurnal waves. The different behaviour of  $K_1$  and  $M_2$  can be explained by the combination of the two phenomena.  $M_2$  is the most affected by the shift in the resonance mode, and therefore suffers a reduction in amplitude when tidal flats are removed.  $K_1$  is affected by both phe-

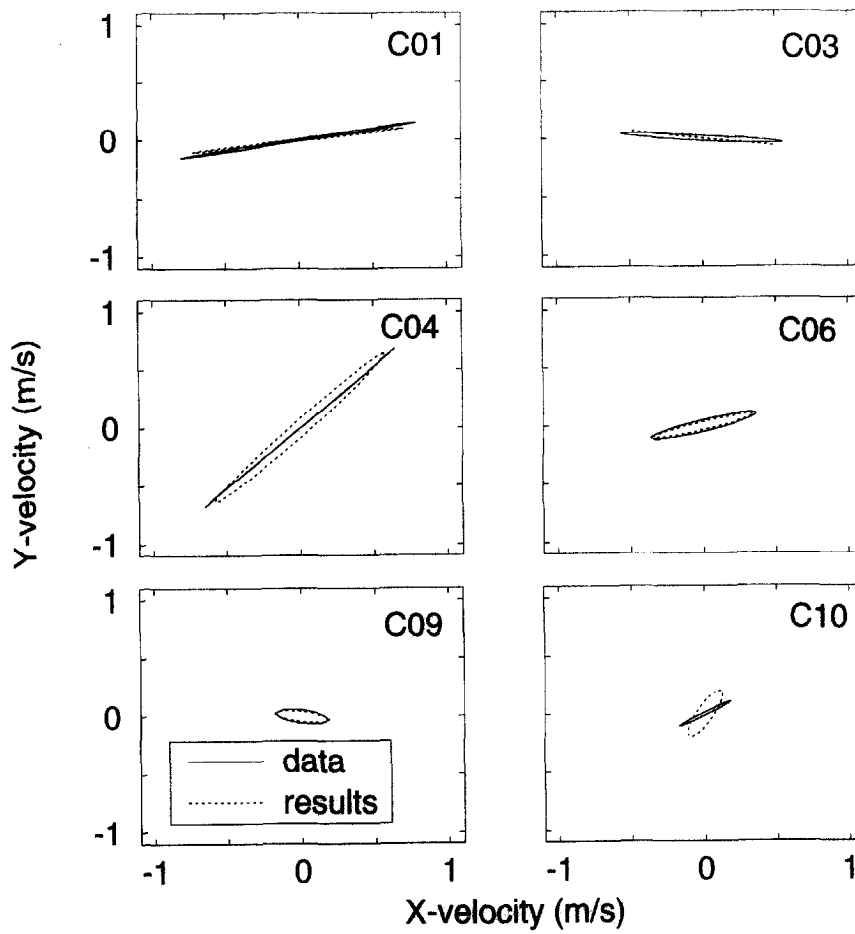


Figure 7.  $M_2$  tidal ellipses at the six velocity stations.

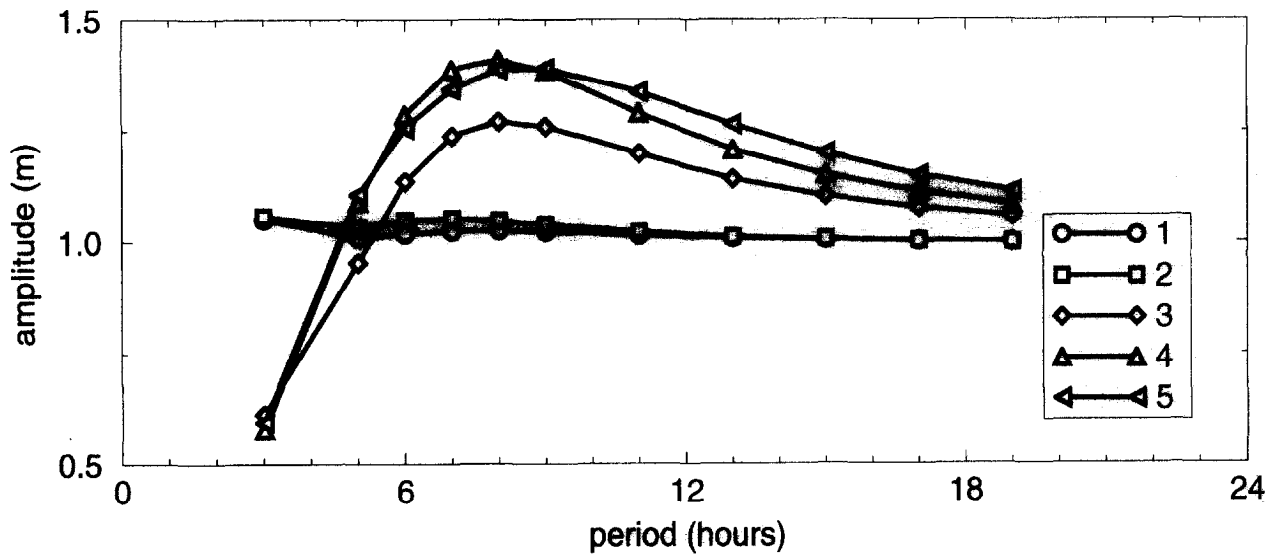
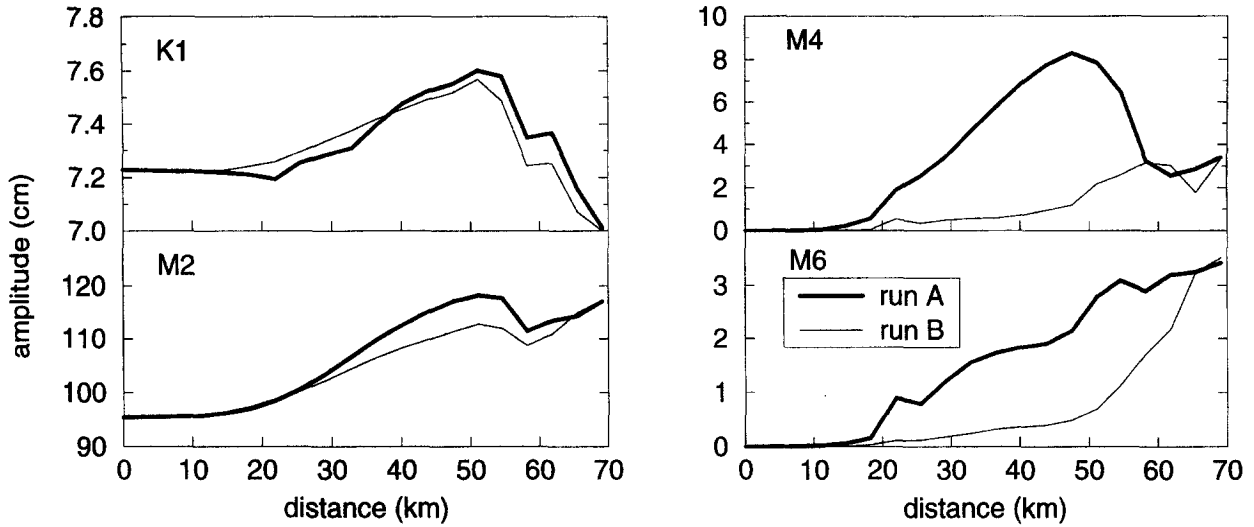


Figure 8. Resonance effects in the Tagus estuary. The locations of the symbols are indicated in figure 2.



**Figure 9.** Amplitudes along the dotted line shown in *figure 2* show the effects of tidal flats on selected frequencies. Run A is the standard simulation, and tidal flats were removed in Run B.

nomena: its amplitude grows in the upper estuary and decreases in the lower estuary. Both changes for  $K_1$  are mild, as the two phenomena oppose each other.

The average difference in duration between ebb and flood was also compared for the two runs in Lisbon. For run A, the difference is comparable with the data (*figure 4*), with the ebbs being shorter than floods by 43 min; for run B, floods are about five minutes shorter than ebbs. These results show that there is a positive feedback between the hydrodynamics and the accretion in the tidal flats. As deposition occurs in the tidal flats, the duration of ebbs increases. The longer ebbs decrease sediment flushing, thus increasing accretion rates. This process is confirmed by field evidence. Accretion rates in the upper estuary were estimated by bathymetric comparisons at  $0.8 \text{ cm y}^{-1}$  between 1928 and 1964, and  $1.7 \text{ cm y}^{-1}$  between 1964 and 1985 [6].

#### 4.2. Energy fluxes

One of the known effects of tidal flats is to dissipate energy: in flood, water spills from the channels into the tidal flats, where it loses momentum due to strong friction; on ebb, the water in the channels is decelerated by mixing with water from the tidal flats, which has little momentum [9]. In order to quantify the energy losses due to tidal flats, we evaluated energy fluxes in the estuary. Depth-integrated energy fluxes are computed as [4]:

$$F = H\rho\left(\frac{1}{2}v^2 + g\eta\right)v \quad (3)$$

where  $g$  is gravity, and the density  $\rho$  was taken as  $1015 \text{ kg m}^{-3}$ .

Yearly-averaged depth-integrated energy fluxes are shown in *figure 10*, and fluxes across selected cross-sections are presented in *table II*. At the river boundary, the net energy flux for the astronomic constituents is directed downstream, which is consistent with the overestimation of frictional dissipation by the model. However, the astronomical tidal energy input into the estuary through the upstream boundary is only 6 % of the input at the mouth of the estuary, and can therefore be neglected.

Energy fluxes across cross-sections (*table II*) show that three-quarters of the energy entering the system are dissipated in three areas: the upper estuary (38 % between sections 5, 6 and 8); the mouth (20 % between sections 1 and 2); and upstream of the main channel (16 % between

**Table II.** Vertically integrated tidal power flux (MW) normal to the cross-sections shown in *figure 10*. Positive values represent upstream fluxes. Astronomic constituents are the diurnal and semi-diurnal; shallow water constituents comprise all others. Note that the flux components do not balance the total flux, due to the non-linearity of Equation (3).

Cross-section	All constituents	Astronomic constituents	Shallow water constituents
1	49.3	52.4	-0.8
2	37.1	40.6	-1.9
3	31.3	35.3	-2.3
4	2.5	3.2	-0.3
5	18.9	23.4	-2.3
6	-5.0	0	-3.0
7	-10.8	-3.1	-5.3
8	0.8	1.2	-0.2

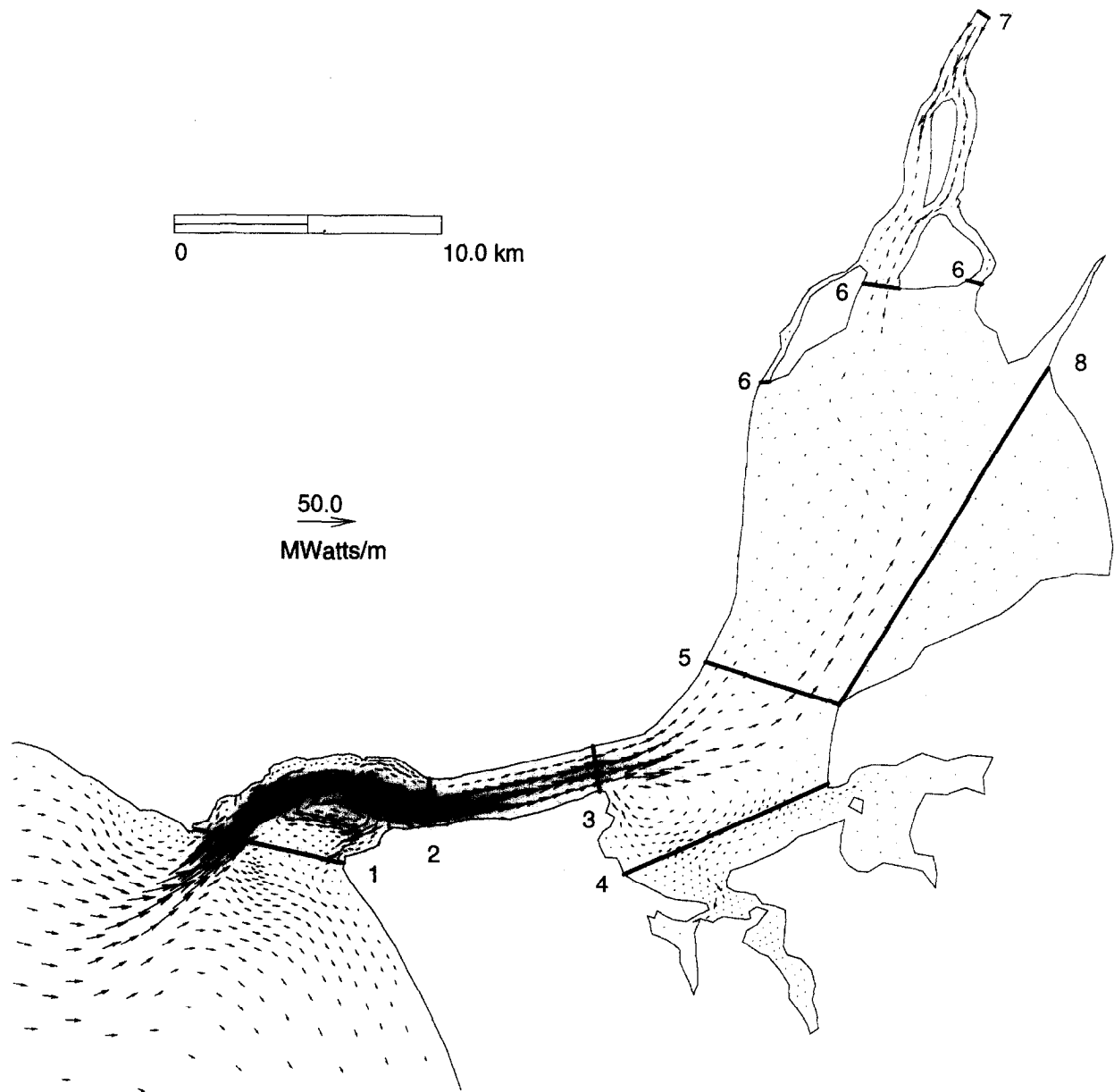


**Figure 10.** Yearly averaged, vertically integrated energy fluxes. Fluxes were interpolated into a coarse grid for clarity. Numbered cross-sections are referenced in *table II* and are used to compute tidal power.

sections 3, 4 and 5). The three regions with extensive tidal flats (the regions southeast of sections 4 and 8) account for only 5 % of the energy dissipation. These results show that the contribution of tidal flats to energy dissipation is negligible, contrary to our expectations: energy is dissipated mostly in shallow channels, and in

regions where large eddies occur. Tidal flats act as filters, transforming energy at astronomic frequencies into energy at non-linear frequencies. The two regions characterized by extensive tidal flats have a net input of energy from astronomic constituents, and a net output in the shallow water constituents.

Finally, it is worth noting the importance of large eddies in dissipating energy, through lateral viscosity effects. The two areas with large residual eddies (between sections 1 and 2, and 3, 4 and 5) account for 36 % of the energy dissipation. Changes in the estuary likely to affect these eddies (e.g. the proposed closing of the Bugio Bank) can therefore have an important impact on the tidal propagation into the estuary.

## 5. SUMMARY AND DISCUSSION

A high-resolution model of tidal propagation in the Tagus estuary was developed, motivated by the need to understand the recent changes in the hydrodynamics. Comparison with field data indicates a major improvement relative to previous modelling efforts, but some errors remain, probably due to limitations in the data.

Results show that tidal flats act as filters, shifting energy from the astronomic frequencies to the non-linear frequencies. Although the energy dissipation in the tidal flats is relatively small (roughly 5 % of the energy input into the system), these shallow areas play an important role in determining the resonance period of the estuary. Removing the tidal flats shifts the resonance period away

from the dominating semi-diurnal frequencies, reducing their amplification in the estuary.

The present trend of accretion in the upper estuary appears to be self-sustained. As the tidal flats become dry land, the reduction of non-linear tidal generation leads to a shift from ebb-dominance (ebbs shorter than floods) to flood-dominance. Tidal velocities will increase on flood, reducing the ability of the system to flush incoming sediments from the river, and eventually leading to an inflow of marine sediments. We can therefore expect that the rate of accretion will increase gradually, and that increasing dredging will be required to maintain the navigation conditions in the estuary. Simultaneously, the extent of the tidal flats will tend to increase.

## Acknowledgements

The authors are grateful to Drs. R.A. Luettich, Jr. and J.J. Westerink for the hydrodynamic model ADCIRC, and to Dr. R. Rodrigues and M. Lacerda for some river data. Suggestions by Mr. P. Elias, Dr. R.A. Luettich, Jr., and two anonymous reviewers are also gratefully acknowledged. The contribution of the second author was partially funded by *Junta Nacional de Investigação Científica e Tecnológica* (BD-2775/93).

## REFERENCES

- [1] Castanheiro J.M., Distribution, transport and sedimentation of suspended matter in the Tejo Estuary, in: estuarine processes: an application to the Tagus Estuary, secretaria de estado do ambiente e recursos naturais, Lisboa (1986) 75–90.
- [2] DGRHA., Monografias hidrológicas dos principais cursos de Água de Portugal continental, direcção geral dos recursos e aproveitamentos hidráulicos, Lisbon, 1986, 569 p (in Portuguese).
- [3] Figueres G., Martin J.M., Meybeck M., Seyler P., A Comparative study of mercury contamination in the Tagus Estuary (Portugal) and major french estuaries (Gironde, Loire, Rhone), Est. Coast. Shelf Sci. 20 (1985) 183–203.
- [4] Foreman M.G.G., Walters R.A., Henry R.F., Keller C.P., Dolling A.G., A tidal model for eastern Juan de Fuca strait and the southern strait of Georgia, J. Geophys. Res. 100, C1 (1995) 721–740.
- [5] Fortunato A.B., Baptista A.M., Luettich, Jr. R.A., A three-dimensional model of tidal currents in the mouth of the Tagus Estuary, Cont. Shelf Res. 17 (14) (1997) 1689–1714.
- [6] Freire P., Andrade C., Evolução sedimentar recente da zona montante do Estuário do Tejo, in actas da 3ª reunião do quaternário Ibérico, Universidade de Coimbra, (1993) 247–255 (in Portuguese).
- [7] Friedrichs C.T., Aubrey D.G., Speer P.E., Impacts of relative sea-level on evolution of shallow estuaries, in Cheng R.T., (ed.) residual currents and long-term transport, Amer. Geophys. Union (1990) 105–122.
- [8] Kolar R.L., Westerink J.J., Cantekin M.E., Blain C.A., Aspects of non-linear simulations using shallow water models based on the wave continuity equation, Computers and fluids, 23 (1994) 523–538.
- [9] Kuo A.Y., Park K., A framework for coupling shoals and shallow embayments with main channels in numerical modeling of coastal plain estuaries, Estuaries 18 (2) (1995) 341–350.
- [10] Luettich Jr. R.A., Westerink J.J., Implementation and testing of elemental flooding and drying in the ADCIRC hydrodynamic model, department of the Army, US Army Corps of Engineers (1995).

- [11] Luetlich Jr. R.A., Westerink J.J., Sheffner N.W., ADCIRC: and advanced three-dimensional model for shelves, coasts and estuaries, report 1: theory and methodology of ADCIRC-2DDI and ADCIRC-3DL, department of the Army, US army corps of engineers (1991).
- [12] Martins M., Galvão T., Figueiredo H., Estudo ambiental do estuário do Tejo-estudo de qualidade de Água-resultados referentes às observações sinópticas de 1982, CAN/TEJO n° 30-REL 27 (1983) (in Portuguese).
- [13] Oliveira I.B.M., Port of Lisbon improvement of the access conditions through the Tagus estuary entrance, in: Proc. Coastal Eng. Conf., ASCE, New York (1993) 2745-2757.
- [14] Portela L.I., Modelação de processos hidrodinâmicos e de qualidade da Água no estuário do Tejo, PhD Thesis, Instituto Superior Técnico, Lisbon (submitted—in Portuguese) (1998) 240 p.
- [15] Rodrigues A.C., Silva P.A., Ferreira V.G., Silva M.C., Um modelo de Apoio à decisão para a Gestão da qualidade de Água na Bacia do Rio Trancão, in: Water quality-assessment and management, PGRIH/T, Lisbon, 109-120 (1989) (in Portuguese).
- [16] Silva M.C., Oliveira E.M., Expo '98: Hydrodynamic modelling of the Tagus Estuary, Rep. 174/95-NET, Laboratório nacional de Engenharia civil, Lisbon, Portugal (in Portuguese) (1995).
- [17] Vale C., Sundby B., Suspended sediment fluctuations in the Tagus Estuary on semi-diurnal and fortnightly time scales, Estuarine, Coast. Shelf Sci. 25 (1987) 495-508.